

Surface Evaluation of Corrosion Test Specimens of Welded AISI 1020 Steel

¹Bambang Yuniarto, ^{2*}Yusuf Umardani, ³Susilo Adi Widyanto, ⁴Agus Suprihanto

^{1,2,3,4}Mechanical Engineering Department, Faculty of Engineering, Diponegoro University, Jl. Prof. H. Soedarto, SH, Tembalang-Semarang 50275, Indonesia

*Corresponding Author's E-mail: umardaniyusuf70@gmail.com

Abstract - The welding process of AISI 1020 steel causes changes in microstructure and corrosion resistance. The corrosion attack pattern occurring on the steel can be evaluated by observing the corroded surface. This research aims to determine the corrosion attack pattern on welded joints of AISI 1020 steel. Specimens of AISI 1020 steel that have been welded and subjected to post-weld heat treatment (PWHT). PWHT involves heating the specimens to temperatures of 400, 500, and 600°C with a holding time of 1 hour, followed by air cooling. The specimens, both before and after PWHT, were tested for corrosion using polarization techniques. The surface of the specimens after corrosion testing was observed using a microscope. The observation results indicate the presence of pitting corrosion on the specimen surfaces after the corrosion test.

Keywords: AISI 1020, PWHT, Corrosion Test.

I. INTRODUCTION

AISI 1020 steel is a low-carbon steel widely used in the construction of building structures [1]. The common method for joining this steel is through Shielded Metal Arc Welding (SMAW) [2]. The low carbon content results in a relatively stable microstructure consisting of ferrite and pearlite phases. However, welding in the Heat-Affected Zone (HAZ) and weld metal leads to changes in grain size, causing microstructural heterogeneity in the vicinity of the weld joint. This heterogeneity contributes to a decrease in corrosion resistance. To restore corrosion resistance, an effort is made to homogenize the microstructure by applying Post-Weld Heat Treatment (PWHT).

PWHT is essentially performed by heating the welded steel to a specific temperature for a certain duration and then cooling it in open air. In addition to homogenizing the microstructure, PWHT can also reduce residual stresses resulting from the welding process. These residual stresses arise due to thermal cycles during welding. If not eliminated, residual stresses can lead to a decrease in corrosion resistance. Therefore, PWHT not only homogenizes the microstructure

but also reduces residual stresses, thereby improving corrosion resistance.

In general, the base metal and HAZ have the same chemical composition, but welding processes lead to differences in grain morphology, including size, shape, and distribution [3]. Meanwhile, the weld metal may have a slightly different chemical composition depending on the welding electrode used [4]. Ideally, for the weld metal to have the same chemical composition as the base metal and HAZ, the welding electrode's chemical composition should match that of the base metal. However, achieving this is challenging because welding electrodes available in the market often have different chemical compositions from the steel being welded.

Due to the potential differences in chemical composition in the weld metal, the corrosion attack pattern in the vicinity of the weld joint differs from that in the base metal and HAZ. This research investigates the corrosion attack pattern in the weld joint area by observing the surface of test specimens before and after corrosion testing using polarization methods.

II. RESEARCH METHOD

A 3mm thick AISI 1020 steel plate was welded using Shielded Metal Arc Welding (SMAW) technique. The welding parameters included a current of 60 A, voltage of 20-26V, welding speed of 38 mm/minute, butt joint design, and welding position of 1G. The welding electrode used is RD460, which complies with AWS A50.1 E6013. Table 1 and Table 2 show the chemical composition of AISI 1020 and welding electrode RD460.

After welding, the plate was flattened using a milling machine. The flattened specimen then underwent a Post-Weld Heat Treatment (PWHT) process. The PWHT process involved heating the specimen using a Euroterm furnace at temperatures of 400, 500, and 600 degrees Celsius for 1, 2, and 4 hours, respectively, followed by cooling in open air.

Before corrosion testing, the specimen's surface was polished gradually using sandpaper with grits 400, 600, 800, 1000, and 1500, and then polished to achieve a shiny surface.

Corrosion testing was conducted using the polarization technique on a potentiostat of the Corrtest CS300 series. The corrosion test solution used was seawater with a primary content of 3.5% NaCl.

The evaluation of corrosion attack is carried out by comparing the surfaces of specimens before and after corrosion testing. Surface observations are conducted using an Olympus brand Light Optical Microscope (LOM) from the BX series.

Table 1: Chemical composition of AISI 1020 (%wt)

C	Si	Mn	P	Fe
0.15 - 0.20	0.20 - 0.24	0.005	0.005	Balance

Table 2: Chemical composition of RD460 electrode (%wt)

C	Si	Mn	Mo	Cr	Ni	V	Fe
0.20	1.00	1.20	0.3	0.20	0.30	0.08	Balance

III. RESULTS AND DISCUSSION

The appearance of the entire specimen surface before undergoing corrosion testing, both before and after PWHT, looks clean. This indicates that the polishing process has resulted in a smooth surface without any scratches that could worsen corrosion attack [5, 6]. The appearance of the entire specimen surface that has undergone corrosion testing, both for specimens subjected to PWHT and those that have not, shows the presence of scattered dark spots.



Figure 1: Surface appearance specimens before PWHT 100x magnification

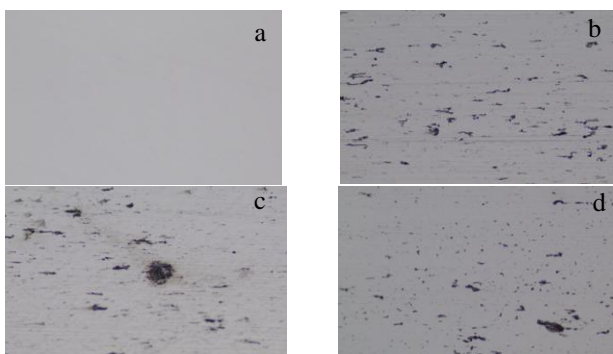


Figure 2: Surface appearance PWHT specimens at 400°C. a) before corrosion test, b, c & d after corrosion test. (b. 1 hr holding time, c. 2 hr holding time & d. 4 hr holding time. 100x magnification)

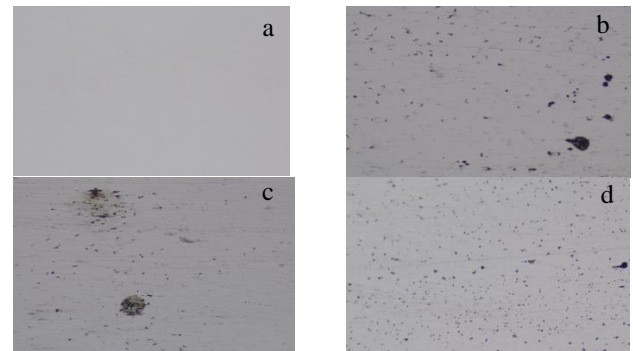


Figure 3: Surface appearance PWHT specimens at 500°C. a) before corrosion test, b, c & d after corrosion test. (b. 1 hr holding time, c. 2 hr holding time & d. 4 hr holding time. 100x magnification)

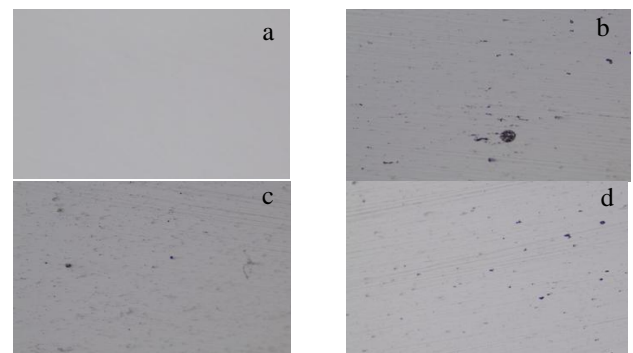


Figure 4: Surface appearance PWHT specimens at 600°C. a) before corrosion test, b, c & d after corrosion test. (b. 1 hr holding time, c. 2 hr holding time & d. 4 hr holding time. 100x magnification)

Figure 1 shows the appearance of specimens before and after corrosion testing without undergoing PWHT. It is observed in Picture 1 that on the specimen's surface after corrosion testing, there are small, elongated dark spots evenly distributed across the entire surface.

Figure 2 depicts the surface of specimens subjected to PWHT at a temperature of 400°C. It is evident that the specimen's surface after corrosion testing still shows dark spots, similar to those in specimens without PWHT. However, the distribution of the dark spots is larger, uneven, and clustered. It is also noticeable that with a longer holding time, the bright-colored areas become more dominant.

PWHT at a temperature of 500°C results in a specimen surface where bright-colored areas are more dominant after corrosion testing. The dark spots become smaller and more evenly distributed. Nevertheless, there are still large dark spots in some areas. Figure 3 show the surface appearance of PWHT specimen at 500°C.

PWHT at a temperature of 600°C indicates that the dark spots on the specimen's surface after corrosion testing become smaller and more evenly distributed. Compared to PWHT at temperatures of 400 and 500°C, PWHT at 600°C results in a specimen surface after corrosion testing that is brighter, with

the smallest dark spots distributed uniformly. Figure 4 show the surface appearance of PWHT specimen at 600oC.

Corrosion testing using the polarization method essentially simulates accelerated corrosion attacks by disrupting the potential equilibrium through the application of overvoltage [8]. Therefore, the appearance of the surface after corrosion testing can provide insights into how corrosion attacks occur on the specimen.

The dark spots seen in the LOM images are an effect of distorted light due to uneven surfaces, not returning to the observer's eyes, resulting in a darker appearance [9]. This indicates that these dark spots are actually holes. The appearance of these dark spots suggests that corrosion attack not only occurs uniformly but also, in specific spots corrosion happens more rapidly.

Corrosion in low-carbon steel is generally dominated by uniform corrosion attacks. However, the presence of heterogeneity in materials such as chemical composition, microstructure, residual stresses, etc., can cause certain areas to experience corrosion more rapidly. Corrosion in low-carbon steel generally does not occur in small spots but in relatively large areas. Therefore, the presence of dark spots indicates the occurrence of localized corrosion, similar to the phenomenon of pitting corrosion in austenitic stainless steel caused by chloride ions. This corrosion is a type of localized corrosion commonly found in stainless steel without molybdenum alloy. Pitting corrosion in stainless steel primarily attacks the Fe metal due to the passive layer of Cr₂O₃ being unable to protect the entire surface of stainless steel from corrosion by chloride ions.

AISI 1020 is a low-alloy carbon steel without other alloying elements besides carbon. Carbon steels, in general, have low corrosion resistance in seawater. This is because the passive iron oxide layer on the surface is not strong and stable enough to inhibit corrosion attack caused by chloride ions.

IV. CONCLUSION

The results of surface observations after corrosion testing on AISI 1020 steel welded using SMAW reveal the presence of dark spots. The dark spot indicates the characteristic of pitting corrosion. The dark spots significantly decrease during PWHT at 600°C with a holding time of 4 hours. In general, as the PWHT temperature increases and the holding time lengthens, the presence of dark spots decreases, both in terms of quantity and size, and their distribution becomes more uniform.

Although the observation results indicate the presence of dark spots indicative of pitting corrosion, unfortunately, the

polarization corrosion testing method only provides data on the corrosion rate for uniform corrosion attacks and cannot measure the corrosion rate due to localized corrosion attacks. Therefore, the corrosion rate data generated needs to be interpreted with caution.

REFERENCES

- [1] Dewangan, S., Selvaray, S. K., Karthikeyan, B., Adane, T. M., Chattopadhyaya, S., Krolczyk, G., Raju, R., 2022, Metallographic Investigation on Postweld Heat Treated 0.21%C-1020 Steel Plates Joined by SMAW Method Advances in Materials Science and Engineering, Volume 2022, 11 pages, <https://doi.org/10.1155/2022/9377591>.
- [2] Rajbhoj, A. B., Diwate, A. D., 2020, Process Parameter Optimization of Sheet Metal Arc Welding of AISI 1020 Mild Steel, Journal of Production and Industrial Engineering, Vol. 1, No. 1, Pafes: 1-11, <https://doi.org/10.26706/jpie.1.1.20200605>.
- [3] Iren E., Civi, C., 2021, The Effect of Welding on Reliability of Mechanical Properties of AISI 1020 and AISI 6150 Steel Materials, Revista De Metalurgia, Vol. 7, No. 1, Pages: 1-11, <https://doi.org/10.3989/revmetalm.186>.
- [4] Khan, M., Dewan, M. W., Sarkar, M.Z., 2021, Effects of welding technique, filler metal and post-weld heat treatment on stainless steel and mild steel dissimilar welding joint, Journal of Manufacturing Processes, Volume 64, Pages 1307-1321, <https://doi.org/10.1016/j.jmapro.2021.02.058>.
- [5] Malik, J., Toor, I. H., Ahmed, W. H., Gasem, Z. M., Habib, M. A., Ben-Mansour, R., Badr, H. M., 2014, Investigation on The Corrosion-Enhanced Erosion Behavior of Carbon Steel AISI 1020, International Journal of Electrochemical Science, Vol. 9, Pages: 6765-6780.
- [6] Ojong, E., Aqua, G. E., Iminabo, J. T., 2021, Effect of Surface Finish on Corrosion and Microstructure of Carbon Steel-(C-1020) and Stainless Steel-(SS304), International Research Journal of Advanced Engineering and Science, Volume 6, Issue 4, pp. 136-145, 2021.
- [7] Roy, S., Nayak, B.B., Sahu, S., 2023, Investigation on the Microstructure–Corrosion Correlation of Commercially Available AISI 1020 and 304 Steel. In: Arockiarajan, A., Duraiselvam, M., Raju, R., Reddy, N.S., Satyanarayana, K. (eds) Recent Advances in Materials Processing and Characterization. Lecture Notes in Mechanical Engineering. Springer, Singapore. https://doi.org/10.1007/978-981-19-5347-7_14.
- [8] Xie, J., Alpas, A.T. & Northwood, D.O., 2003, The Effect Of Erosion On The Electrochemical Properties

- Of AISI 1020 Steel. Journal of Materials Engineering and Performance, Vol. 12, Pages: 77–86, <https://doi.org/10.1361/105994903770343510>.
- [9] Hong, H., Yang, S., 1997, A new light optical metallographic technique for revealing grain structures of common 2000, 5000, and 7000 series aluminum alloys, Materials Characterization, Vol. 38, No. 3, Pages 165-175, [https://doi.org/10.1016/S1044-5803\(97\)00040-5](https://doi.org/10.1016/S1044-5803(97)00040-5).
- [10] Mudali, U. K., Pujar, M. G., 2002, 3 - Pitting Corrosion of Austenitic Stainless Steels and Their Weldments, Editor(s): H.S. Khatak, Baldev Raj, In Woodhead Publishing Series in Metals and Surface Engineering, Corrosion of Austenitic Stainless Steels, Woodhead Publishing, Pages 74-105, <https://doi.org/10.1533/9780857094018.106>.

Citation of this Article:

Bambang Yunianto, Yusuf Umardani, Susilo Adi Widyanto, Agus Suprihanto, “Surface Evaluation of Corrosion Test Specimens of Welded AISI 1020 Steel” Published in *International Research Journal of Innovations in Engineering and Technology - IRJIET*, Volume 7, Issue 11, pp 585-588, November 2023. Article DOI <https://doi.org/10.47001/IRJIET/2023.711077>
